nature materials

LETTERS

PUBLISHED ONLINE: 17 JULY 2011 | DOI: 10.1038/NMAT3065

Kinetics of non-equilibrium lithium incorporation in $LiFePO_4$

Rahul Malik[1], Fei Zhou[2] and G. Ceder[1]*

Lithium-ion batteries are a key technology for multiple clean energy applications. Their energy and power density is largely determined by the cathode materials, which store Li by incorporation into their crystal structure. Most commercialized cathode materials, such as $LiCoO_2$ (ref. 1), $LiMn_2O_4$ (ref. 2), $Li(Ni, Co, Al)O_2$ or $Li(Ni, Co, Mn)O_2$ (ref. 3), form solid solutions over a large concentration range, with occasional weak first-order transitions as a result of ordering[1] of Li or electronic effects[4]. An exception is $LiFePO_4$, which stores Li through a two-phase transformation between $FePO_4$ and $LiFePO_4$ (refs 5–8). Notwithstanding having to overcome extra kinetic barriers, such as nucleation of the second phase and growth through interface motion, the observed rate capability of $LiFePO_4$ has become remarkably high[9–11]. In particular, once transport limitations at the electrode level are removed through carbon addition and particle size reduction, the innate rate capability of $LiFePO_4$ is revealed to be very high. We demonstrate that the reason $LiFePO_4$ functions as a cathode at reasonable rate is the availability of a single-phase transformation path at very low overpotential, allowing the system to bypass nucleation and growth of a second phase. The Li_xFePO_4 system is an example where the kinetic transformation path between $LiFePO_4$ and $FePO_4$ is fundamentally different from the path deduced from its equilibrium phase diagram.

In the considerable volume of literature on the subject, the lithiation mechanism in (Li)$FePO_4$ is conventionally described and interpreted as a two-phase growth process[12–18] involving the coexistence of both phases ($LiFePO_4$ and $FePO_4$), initiated by a nucleation event. According to classical nucleation theory, on lithiation of $FePO_4$ the inserted Li will pool together to form clusters, which only grow once a critical size is reached. The critical size, below which the new phase dissolves again, exists because the driving force for transformation scales with volume, and the interfacial energy which hinders the transformation scales with area. These concepts lead to the well-known expressions for the critical radius ($r*$) and critical nucleation barrier (ΔG_{r*}), $r* = 2\gamma \cdot v/(|\phi| - \Delta g_s)$ and $\Delta G_{r*} = 16\pi \cdot \gamma^3 \cdot v^2/3(|\phi| - \Delta g_s)^2$ (ref. 19), where γ is the $LiFePO_4/FePO_4$ interfacial energy, v is the $LiFePO_4$ molar volume, ϕ is the applied underpotential, and Δg_s is the coherency strain energy. Using values determined from first-principles calculations of the interfacial energy[20] ($\gamma = 0.96\,J\,m^{-2}$) and coherency strain energy[21] ($\Delta g_s \approx 3{,}200\,J\,mol^{-1}$ or 33 meV/Li for nucleating $LiFePO_4$ in 'morphology 1' in ref. 21) available in the literature, $r*$ and ΔG_{r*} can be determined as a function of the applied underpotential. For a critical nucleus to be smaller than 100 nm (that is for $r* = 50$ nm), which is a typical size of a primary $LiFePO_4$ particle in a composite electrode, an underpotential in excess of 50 mV must be applied, and ΔG_{r*} is at least several hundred thousand kT (thermal energy) at room temperature per cluster. This very large energy required to form the critical nucleus makes nucleation very unlikely. Even if one were to ignore the coherency strain energy altogether, and reduce the interfacial energy by a factor of two (for example, to account for heterogeneous nucleation), ΔG_{r*} for a 50 nm diameter nucleus exceeds 300,000 kT per cluster. Considering this very large ΔG_{r*}, and the fact that the voltage hysteresis between charge and discharge in very slow discharging experiments (C/1,000) approaches only ~20 mV (ref. 22), the lithiation mechanism in $LiFePO_4$ is clearly inadequately described by classical nucleation and growth. An identical analysis performed here applies to the charging procedure.

If nucleation does not proceed then the Li_xFePO_4 and $Li_{1-x}FePO_4$ solid solutions can be highly oversaturated. To investigate the energetics of metastable solid solutions in Li_xFePO_4 as an alternative transformation path, we have used the cluster expansion approach combined with *ab initio* density functional theory calculations[23]. The cluster expansion allows determination of the energy of any Li/vacancy and Fe^{2+}/Fe^{3+} configuration in the system, and was parametrized from the calculated energies of 245 different Li/vacancy and electron/hole configurations in Li_xFePO_4 ($0 \le x \le 1$) shown in Fig. 1a. These same formation energies were used previously as input to Monte Carlo simulations to accurately reproduce the Li_xFePO_4 phase diagram[7]. As shown in Fig. 1a, no Li_xFePO_4 states with intermediate Li concentration ($0 < x_{Li} < 1$) have negative formation energies, in agreement with low-temperature phase separation. However, at several compositions between $x_{Li} = 0$ and $x_{Li} = 1$ the formation energies are very low, and well below kT at room temperature: for instance 10.6 meV per formula unit at $x_{Li} = 0.333$, 5.2 meV per formula unit at $x_{Li} = 0.833$, and 5.1 meV per formula unit at $x_{Li} = 0.667$. Of the 245 formation energies shown in Fig. 1a, 96 are below kT. This suggests that with minimal energy added to the system an insertion path that traverses through intermediate Li_xFePO_4 structures is possible. The advantages of a single-phase transformation path are significant: not only is the transformation facile, but lithiation of the particles is more homogeneous than in the two-phase model, thus reducing stresses and possible mechanical degradation of the material, consistent with the excellent cycling behaviour of $LiFePO_4$ electrodes.

To better quantify the free energy and voltage along a metastable transformation path, we performed canonical Monte Carlo simulations with the $LiFePO_4$ cluster expansion[7], with appropriate constraints to avoid phase separation, to obtain the free energy of non-equilibrium states. Specifically, we used small

[1]Department of Materials Science and Engineering, Massachusetts Institute of Technology, 77 Massachusetts Avenue, Cambridge, Massachusetts 02139, USA, [2]Department of Materials Science and Engineering, University of California, Los Angeles, California 90095, USA. *e-mail: gceder@mit.edu.

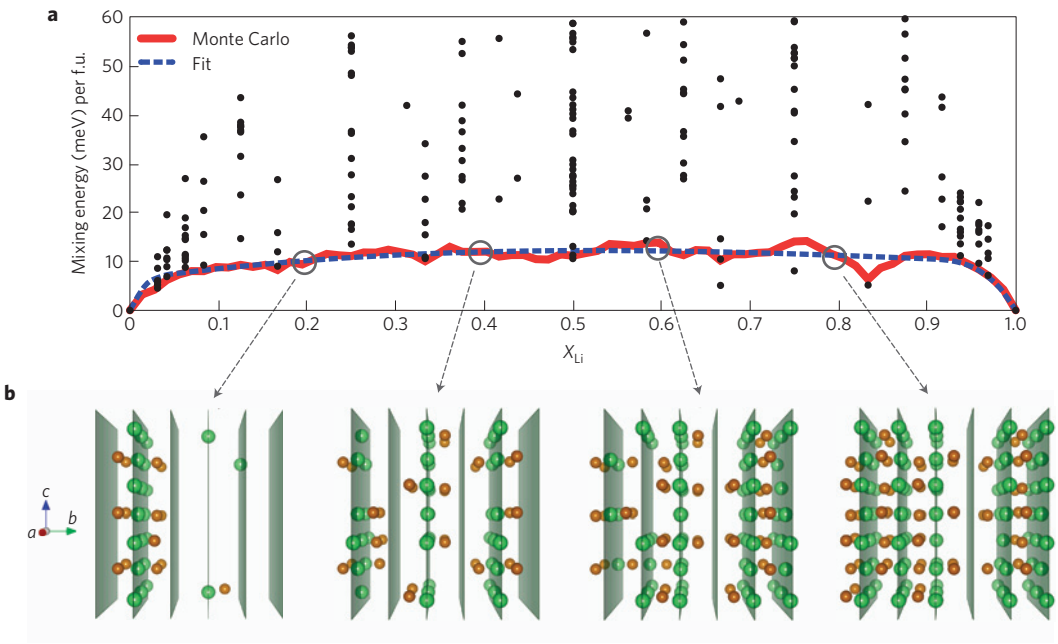

Figure 1 | Free energy and atomic configurations along the single-phase $LiFePO_4$ transformation path. a, Zero-temperature mixing energies (black circles) calculated from first principles of 245 different Li/vacancy and electron/hole configurations in Li_xFePO_4 ($0 \leq x \leq 1$) show the existence of several low formation energy structures. The non-equilibrium free energy curve at room temperature determined by canonical Monte Carlo simulations (solid red) using small simulation cells ($2 \times 3 \times 3$ unit cells), as well as the least squares cubic spline fit of the Monte Carlo data (dashed blue) both plateau at ~15 meVper formula unit (f.u.) within $\sim 0.05 < x_{Li} < 0.9$. **b**, Snapshots of Li (green atoms) and Fe^{2+} (brown atoms) configurations in Monte Carlo simulations at room temperature for $x_{Li} = 0.2, 0.4, 0.6, 0.8$ show the succession of single-phase states with some local ordering. Adjacent (010) planes containing Li/vacancy are shown in green.

simulation cells ($2 \times 3 \times 3$ unit cells) for which the phase-separated state is penalized (as an interface would constitute too large a relative contribution to the energy) and non-equilibrium but low energy single-phase states can be captured. The free energy of these states at room temperature is shown in red in Fig. 1a, and a sample of the structures found in the Monte Carlo simulations is shown in Fig. 1b. Several unexpected observations can be made from Fig. 1. First, the free energy does not have the typical regular solution form with two minima separated by a maximum, as is typically assumed in simplified models of $LiFePO_4$, and second, the Li-states, although disordered, show considerable short-range ordering. Specifically, as seen in Fig. 1b, at all concentrations, Li vacancies prefer to accumulate locally within sheets in the *ac* plane (shown in green in Fig. 1b, (010) planes in Miller indices) when possible, leaving the remaining interspersed sheets partially occupied by Li. Local ordering of Li and Li-vacancies has been directly observed experimentally, lending validity to our free energy model shown in Fig. 1a (ref. 24). Overall, the Li ions are distributed equally among the 1D diffusion channels oriented along the [010] direction[25] and, because the Li insertion reaction is a topotactic process, these structures define a continuous lithiation path where all 1D diffusion channels, not just those at a two-phase interface, are simultaneously active in either lithium insertion or deinsertion.

The applied overpotential required to access these states is reflected in the slope of the free energy curve (that is, the Li chemical potential, μ_{Li}), where ΔG is the excess free energy over the equilibrium two-phase free energy:

$$\Delta\phi_{Li} = -\Delta\mu_{Li} = -\left(\frac{\partial \Delta G}{\partial x_{Li}}\right)_T \quad (1)$$

Because the free energy curve in Fig. 1a corresponds to a non-equilibrium path, there will be an inherent voltage hysteresis between charge and discharge, regardless of rate, as seen in slow charge/discharge experiments[22]. Also, the free energy curve is almost flat for the bulk of the concentration range ($\sim 0.05 < x_{Li} < 0.9$), which has remarkable consequences on the charging and discharging behaviour: if the local concentration of Li within a particle is within this range, very little change in driving force (potential) is required to drive either further lithiation or delithiation while avoiding phase separation. Hence, the voltage curve of this solid solution path will be remarkably flat. This is shown clearly in Fig. 2, where the single-particle voltage defined in equation (1) (and obtained from the least squares cubic spline fit of the Monte Carlo solid solution free energy shown in Fig. 1a) is plotted in this specified concentration range. The calculated voltage hysteresis is very small, about 30 mV, which is consistent with Dreyer's observation that the voltage hysteresis in the zero current limit is small, about ~20 mV in $LiFePO_4$ (ref. 22).

The free energy curve in Fig. 1a explains why (de)lithiation of (Li)$FePO_4$ is so facile. Taking discharge (lithiation) as an example, once a very small amount of Li is inserted in a particle (<5%), lithiation will proceed as long as the potential is ~20 mV (the slope of the free energy curve) below the equilibrium potential. As no potential change is required to traverse the composition between $x \approx 0.05$ and $x \approx 0.9$, lithiation will proceed rapidly once a particle has some Li content ($> \approx 0.05$). Besides providing a rationale for the very high rate capability of $LiFePO_4$, our finding of the solid solution path as the most likely transformation path is consistent with several unexplained findings in the material. Several researchers have shown that solid solutions in Li_xFePO_4 created at high T and quenched to room temperature can persist for hours and even days without transforming to their equilibrium two-phase state[5,26–28]. Note that these results are surprising because the Li mobility in these materials is high, as demonstrated both from theoretical results[25] and from its high-rate behaviour[9–11]. The sluggish phase separation observed in these experiments is now explained well by considering the extremely flat solid solution

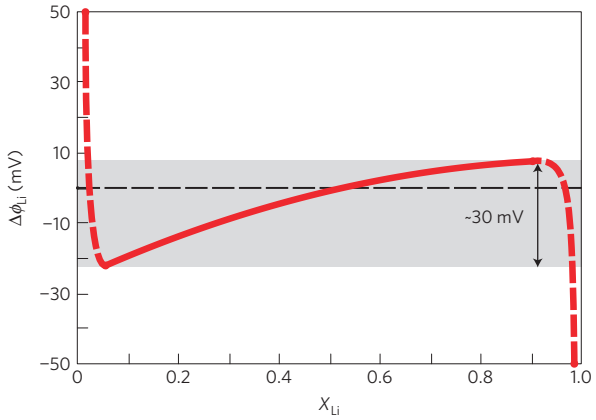

Figure 2 | The single-particle voltage within ~0.05 < x_{Li} < 0.9 defined in equation (1) and obtained from the least squares cubic spline fit of the Monte Carlo data shown in Fig. 1a. The difference between the local maximum and minimum in this curve is the voltage hysteresis[22], indicating negligible voltage polarization between charge and discharge, in good agreement with experimental work[22]. Dashed portions of the curve are drawn to reflect the effect of configurational entropy on the potential in the dilute Li concentration and dilute vacancy limit.

free energy curve in Fig. 1a indicating negligible thermodynamic driving force for demixing.

Although our results indicate that Li_xFePO_4 may transform through a single-phase path, rather than by nucleation and growth of the second phase, the equilibrium state is undoubtedly two-phase. Hence, a partially (dis)charged electrode at rest will relax to the equilibrium two-phase state of lithiated and delithiated $LiFePO_4$, as shown in Fig. 3. Whether the lithiated and delithiated phases coexist within the same particle or as an assembly of particles, each either fully lithiated and delithiated, will vary as a function of particle size, as described by Wagemaker *et al.*[20], with larger particles stabilizing intraparticle two-phase coexistence (Fig. 3b) and smaller particles favouring interparticle two-phase coexistence (Fig. 3a), as observed by Delmas and colleagues[18].

The metastable free energy curve and its associated single particle voltage profile, which we derived from *ab initio* computations, also has significant consequences for the (de)lithiation of a multi-particle assembly, as is the case in a real electrode. The critical step for a particle to transform is to reach a certain concentration (≈0.05 in discharge and ≈0.9 in charge). Once this concentration is reached (de)lithiation proceeds with only a small under(over)potential present. The particles that reach this solid solution regime first will insert (remove) Li as rapidly as their diffusion and surface transfer kinetics allow, even at the expense of nearby particles that have not yet reached this limit. Particle size will play a role in this process, as smaller particles are saturated more rapidly and thus probably transform first. In the large particle limit, Li transport may become diffusion limited, and phase-separation may occur within a particle. Whether the Li is obtained from the electrolyte or from extracting Li from neighbouring particles depends on the relative rate at which Li from these two sources is available. Conversion of some $LiFePO_4$ to $FePO_4$ during discharge (lithiation) has actually been observed in *in situ* X-ray diffraction (XRD) experiments[29]. Overall, this leads to a very inhomogeneous charge/discharge picture of the electrode, where particles will appear either fully lithiated or fully delithiated, as observed by Delmas and colleagues[18]. Delayed and inhomogeneous transformations of $LiFePO_4/FePO_4$ have indeed been observed in multiple *in situ* XRD experiments[29].

In summary, we have shown that, despite its strong two-phase equilibrium character, the remarkable rate capability of $LiFePO_4$ can be explained by the existence of an alternative single-phase

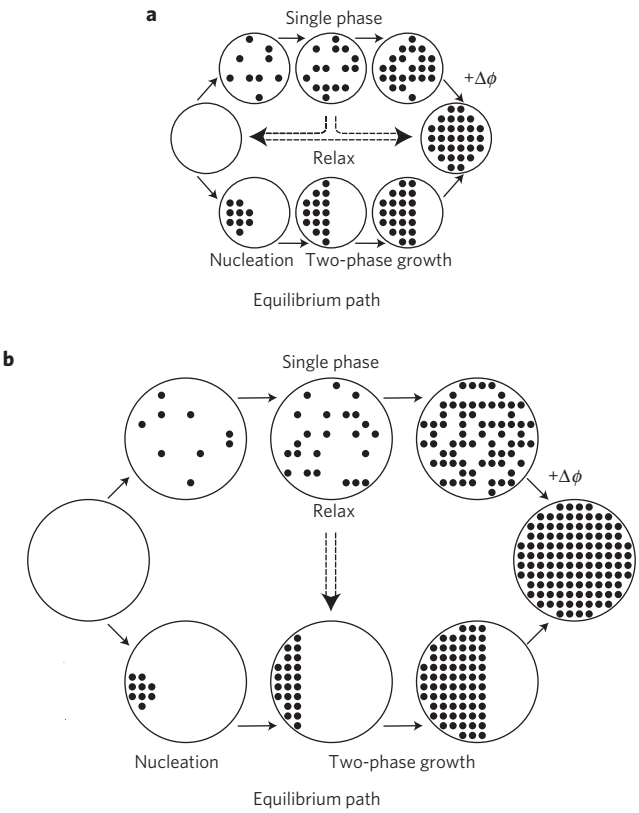

Figure 3 | Comparison of equilibrium and non-equilibrium lithiation in $LiFePO_4$. a,b, Schematic depiction of lithiation via an equilibrium two-phase path (bottom path) characterized by nucleation and growth compared with an alternative non-equilibrium single phase path (upper path) enabled by underpotential $\Delta\phi$ shown for small particles (**a**) and larger particles (**b**). Once the underpotential is removed the system relaxes to the equilibrium state.

transformation path available at very low overpotential, the availability of which obviates the need for nucleation and growth. We have calculated the magnitude of the overpotential needed to enable the single-phase transformation path and determined that only minimal overpotential is required at room temperature. Although $LiFePO_4$ is an example where the transformation path is fundamentally different from the equilibrium thermodynamic behaviour, this result also opens up a more rational approach to the search for new electrode materials. Many potentially new Li-storage materials have strong first-order kinetics in their phase transformations, and often exhibit very poor kinetics[30]. Our work shows that efforts to find new high energy-density materials with reasonable rate capability may have to focus on the potential non-equilibrium paths that are available to the system in a small range of overpotential, as they may be substantially faster than, and different from, the equilibrium path. Such solid–solution non-equilibrium paths can only exist if the phases are topotatically related and if the formation enthalpy of the states with intermediate lithium content is not too high.

Received 9 August 2010; accepted 9 May 2011; published online 17 July 2011

References

1. Reimers, J. N. & Dahn, J. R. Electrochemical and *in situ* X-ray-diffraction studies of lithium intercalation in Li_xCoO_2. *J. Electrochem. Soc.* **139,** 2091–2097 (1992).
2. Thackeray, M. M., Johnson, P. J., Depicciotto, L. A., Bruce, P. G. & Goodenough, J. B. Electrochemical extraction of lithium from $LiMn_2O_4$. *Mater. Res. Bull.* **19,** 179–187 (1984).

3. Ohzuku, T. & Makimura, Y. Layered lithium insertion material of $LiCo_{1/3}Ni_{1/3}Mn_{1/3}O_2$ for lithium-ion batteries. *Chem. Lett.* **30,** 642–643 (2001).
4. Menetrier, M., Saadoune, I., Levasseur, S. & Delmas, C. The insulator–metal transition upon lithium deintercalation from $LiCoO_2$: Electronic properties and Li-7 NMR study. *J. Mater. Chem.* **9,** 1135–1140 (1999).
5. Delacourt, C., Poizot, P., Tarascon, J. M. & Masquelier, C. The existence of a temperature-driven solid solution in Li_xFePO_4 for $0 <= x <= 1$. *Nature Mater.* **4,** 254–260 (2005).
6. Dodd, J. L., Yazami, R. & Fultz, B. Phase diagram of $Li_{(x)}FePO_4$. *Electrochem. Solid State Lett.* **9,** A151–A155 (2006).
7. Zhou, F., Maxisch, T. & Ceder, G. Configurational electronic entropy and the phase diagram of mixed-valence oxides: The case of Li_xFePO_4. *Phys. Rev. Lett.* **97,** 155704 (2006).
8. Yamada, A. *et al.* Room-temperature miscibility gap in Li_xFePO_4. *Nature Mater.* **5,** 357–360 (2006).
9. Chung, S. Y., Bloking, J. T. & Chiang, Y. M. Electronically conductive phospho-olivines as lithium storage electrodes. *Nature Mater.* **1,** 123–128 (2002).
10. Kang, B. & Ceder, G. Battery materials for ultrafast charging and discharging. *Nature* **458,** 190–193 (2009).
11. Kim, D. H. & Kim, J. Synthesis of $LiFePO_4$ nanoparticles in polyol medium and their electrochemical properties. *Electrochem. Solid State Lett.* **9,** A439–A442 (2006).
12. Allen, J. L., Jow, T. R. & Wolfenstine, J. Kinetic study of the electrochemical $FePO_4$ to $LiFePO_4$ phase transition. *Chem. Mater.* **19,** 2108–2111 (2007).
13. Padhi, A., Nanjundaswamy, K. & Goodenough, J. Phospho-olivines as positive-electrode materials for rechargeable lithium batteries. *J. Electrochem. Soc.* **144,** 1188–1194 (1997).
14. Srinivasan, V. & Newman, J. Discharge model for the lithium iron-phosphate electrode. *J. Electrochem. Soc.* **151,** A1517–A1529 (2004).
15. Wang, C., Kasavajjula, U. S. & Arce, P. E. A discharge model for phase transformation electrodes: Formulation, experimental validation, and analysis. *J. Phys. Chem. C* **111,** 16656–16663 (2007).
16. Laffont, L. *et al.* Study of the $LiFePO_4/FePO_4$ two-phase system by high-resolution electron energy loss spectroscopy. *Chem. Mater.* **18,** 5520–5529 (2006).
17. Chen, G. Y., Song, X. Y. & Richardson, T. J. Electron microscopy study of the $LiFePO_4$ to $FePO_4$ phase transition. *Electrochem. Solid State Lett.* **9,** A295–A298 (2006).
18. Delmas, C., Maccario, M., Croguennec, L., Le Cras, F. & Weill, F. Lithium deintercalation in $LiFePO_4$ nanoparticles via a domino-cascade model. *Nature Mater.* **7,** 665–671 (2008).
19. Porter, D. A. & Easterling, K. E. *Phase Transformations in Metals and Alloys* 2nd edn (CRC, 2004).
20. Wagemaker, M., Mulder, F. M. & Van der Ven, A. The role of surface and interface energy on phase stability of nanosized insertion compounds. *Adv. Mater.* **21,** 2703–2709 (2009).
21. Van der Ven, A., Garikipati, K., Kim, S. & Wagemaker, M. The role of coherency strains on phase stability in Li_xFePO_4: Needle crystallites minimize coherency strain and overpotential. *J. Electrochem. Soc.* **156,** A949–A957 (2009).
22. Dreyer, W. *et al.* The thermodynamic origin of hysteresis in insertion batteries. *Nature Mater.* **9,** 448–453 (2010).
23. Zhou, F., Cococcioni, M., Kang, K. & Ceder, G. The Li intercalation potential of $LiMPO_4$ and $LiMSiO_4$ olivines with M = Fe, Mn, Co, Ni. *Electrochem. Commun.* **6,** 1144–1148 (2004).
24. Gu, L. *et al.* Direct observation of lithium staging in partially delithiated $LiFePO_4$ at atomic resolution. *J. Am. Chem. Soc.* **133,** 4661–4663 (2011).
25. Morgan, D., Van der Ven, A. & Ceder, G. Li conductivity in Li_xMPO (M = Mn, Fe, Co, Ni) olivine materials. *Electrochem. Solid State Lett.* **7,** A30–A32 (2004).
26. Delacourt, C., Rodriguez-Carvajal, J., Schmitt, B., Tarascon, J. M. & Masquelier, C. Crystal chemistry of the olivine-type Li_xFePO_4 system ($0 <= x <= 1$) between 25 and 370 °C. *Solid State Sci.* **7,** 1506–1516 (2005).
27. Chen, G., Song, X. & Richardson, T. J. Metastable solid-solution phases in the $LiFePO_4/FePO_4$ system. *J. Electrochem. Soc.* **154,** A627–A632 (2007).
28. Dodd, J., Yazami, R. & Fultz, B. Phase diagram of $Li_{(x)}FePO_4$. *Electrochem. Solid State* **9,** A151–A155 (2006).
29. Chang, H. H. *et al.* Study on dynamics of structural transformation during charge/discharge of $LiFePO_4$ cathode. *Electrochem. Commun.* **10,** 335–339 (2008).
30. Dominko, R., Conte, D. E., Hanzel, D., Gaberscek, M. & Jamnik, J. Impact of synthesis conditions on the structure and performance of Li_2FeSiO_4. *J. Power Sources* **178,** 842–847 (2008).

Acknowledgements

This work was supported as part of the Northeastern Center for Chemical Energy Storage, an Energy Frontier Research Center funded by the US Department of Energy, Office of Science, Office of Basic Energy Sciences under Award Number DE-SC0001294. The electronic structure work enabling this work was funded by the Department of Energy, Office of Basic Energy Science, Grant No. DE-FG02-96ER4557. The authors thank the National Partnership for Advanced Computing Infrastructure (NPACI) for computational resources. The authors would like to acknowledge A. Abdellahi, M. Z. Bazant, C. P. Grey and A. Van der Ven for their helpful discussions and comments.

Author contributions

R.M. and G.C. developed the model and wrote the manuscript. R.M. performed Monte Carlo simulations. F.Z. performed DFT calculations.

Additional information

The authors declare no competing financial interests. Reprints and permissions information is available online at http://www.nature.com/reprints. Correspondence and requests for materials should be addressed to G.C.